Current Research in Food Science 9 (2024) 100898

Contents lists available at ScienceDirect

Current Research in Food Science

journal homepage: www.sciencedirect.com/journal/current-research-in-food-science

Sturgeon-derived peptide LLLE alleviates colitis via regulating gut microbiota and its metabolites

Jie Lin [a,1], Jiani Yang [b,1], Leqi Cui [a], Ravinder Nagpal [a], Prashant Singh [a], Gloria Salazar [a], Qinchun Rao [a], Ye Peng [a], Quancai Sun [a,*]

[a] Department of Health, Nutrition and Food Sciences, Florida State University, Tallahassee, FL, United States
[b] School of Food and Biological Engineering, Jiangsu University, 212013, Zhenjiang, Jiangsu Province, China

ARTICLE INFO

Keywords:
Sturgeon
Anti-inflammatory peptide
Colitis
Bacteroidetes
Metabolites

ABSTRACT

Inflammatory bowel disease (IBD), encompassing ulcerative colitis (UC) and Crohn's disease, entails chronic inflammation of the gastrointestinal tract. The pathogenesis of IBD implicates genetic factors, gut microbiome alterations, and immune dysregulation, contributing to its increasing global prevalence. The sturgeon-derived peptide, which exhibits promising anti-inflammatory effects, provides potential therapeutic insights for managing IBD symptoms. This study aims to elucidate the therapeutic mechanisms of novel sturgeon-derived peptide (LLLE, Leu-Leu-Leu-Glu) by investigating their effects on intestinal inflammation, gut microbiota composition, and fecal metabolites in a mouse model of IBD. LLLE administration alleviated weight loss and disease activity index (DAI) scores in dextran sulfate sodium salt (DSS)-induced colitis in mice. Histopathological examination showed LLLE pretreatment improved colon morphology and histopathological condition and decreased serum interleukin-6 (IL-6) levels. 16S rRNA sequencing indicated LLLE-modulation of gut microbiota, especially alleviated DSS-elevated *Bacteroidetes*. Fecal metabolomic analysis unveiled that LLLE restores critical metabolites such as indole-3-propionic acid, which is pivotal in anti-inflammatory responses. Altogether, sturgeon peptide exhibits considerable promise as a therapeutic agent for colitis, owing to its anti-inflammatory effects, modulation of gut microbiota, and restoration of essential fecal metabolites.

1. Introduction

Inflammatory bowel disease (IBD) is an immune disorder caused by chronic inflammation of the gastrointestinal tract, including ulcerative colitis (UC) and Crohn's disease (Hoon et al., 2018). The pathogenesis of IBD remains unclear and is hypothesized to result from the interplay between genetic factors, the gut microbiome, and immune dysregulation (Ghouri et al., 2020; Nagao-Kitamoto et al., 2016). Although the underlying mechanisms by which gut bacteria contribute to the development of IBD are still unknown, increasing evidence underscores the crucial role of the gut microbiome in the onset of the disease. Alterations in the composition and diversity of the gut microbiota have been observed in IBD patients compared to healthy individuals (Matsuoka and Kanai, 2015). Clinical studies have found a decrease in the overall gut microbiota diversity of IBD patients and a decrease in the abundance of bacteria with anti-inflammatory properties, such as *Suterella*, *Clostridium groups IV* and *XIVa*, *Bifidobacterium* spp., *Feacalibacterium prausnitzii*, and *Roseburia*, as well as an increase in the abundance of colicogenic microbiota such as adherent invasive *Fusobacterium* spp., *E. coli*, *Ruminococcus gnavus*, *Veillonellaceae*, and *Pasteurellaceae* (Knox et al., 2019; Sartor and Wu, 2017). Metabolomics entails identifying and quantifying small to medium-sized molecular metabolites in biological samples. Assessing metabolite levels can reveal normal or altered metabolites or metabolic pathways, advancing our understanding and

Abbreviations: IBD, Inflammatory bowel disease; UC, Ulcerative colitis; LLLE, Leu-Leu-Leu-Glu; DAI, Disease activity index; DSS, Dextran sulfate sodium salt; IL-6, Interleukin-6; NO, Nitric oxide; IL-10, Interleukin-10; CMC, Carboxymethyl cellulose; H&E, Hematoxylin and eosin; ELISA, Enzyme-linked immunosorbent assay; PCoA, Principal coordinate analysis; LEfSe, Linear discriminant analysis effect size; FC, Fold change; VIP, Variable importance in the projection; OPLS-DA, Orthogonal partial least squares-discriminant analysis; TNBS, Trinitrobenzene sulfonic acid; MCP-1, Monocyte chemoattractant protein-1; TNF-α, Tumor necrosis factor-alpha; IL-1β, Interleukin-1 beta; PXR, Pregnane X receptor; AhR, Aryl hydrocarbon receptor.

* Corresponding author.
E-mail address: qsun@fsu.edu (Q. Sun).
[1] These authors contributed equally to the current work.

https://doi.org/10.1016/j.crfs.2024.100898
Received 22 August 2024; Received in revised form 28 September 2024; Accepted 25 October 2024
Available online 28 October 2024

Table 1
DAI score from weight loss, stool consistency, and bleeding. The DAI score is calculated as the sum of these three parameters.

Score	Body weight decrease (%)	Stool consistency	Bleeding daily
0	None	Normal	Normal
1	1–5%	Loose stools	Slight bleeding
2	5–10%		
3	10–20%		
4	>20%	Watery diarrhea	Gross bleeding

diagnosis of diseases (Teckchandani et al., 2021). Therefore, it is essential to elucidate changes in the levels of intestinal flora and their metabolites.

Marine fish are an excellent source of bioactive peptides, typically comprising 3 to 20 amino acid residues (Venkatesan et al., 2017). Our previous studies have concentrated on novel peptides from fish protein hydrolysates derived from fish by-products and waste materials (Gao et al., 2021, 2024; Yuan et al., 2023). Such fish-derived peptides have a variety of biological activities, including antibacterial, antioxidant, antithrombotic, antiprotozoal, anti-obesity, antihypertensive activities and anticancer, immunomodulatory activities and other biological functions, which are very beneficial to human health (Shaik and Sarbon, 2022; Yaghoubzadeh et al., 2020). Based on prior research, we have discovered four novel peptides derived from alcohol-soluble sturgeon cartilage hydrolysates (Yuan et al., 2021, 2023). Among these, LLLE (Leu-Leu-Leu-Glu) has been shown to reduce the production of nitric oxide (NO) and IL-6 while simultaneously increasing interleukin-10 (IL-10) levels in an in vitro cell model (Yuan et al., 2023). Previous experiments suggested that LLLE may have anti-inflammatory potential, and thus, we synthesized LLLE to investigate whether it has an anti-colitis effect. Therefore, this study aimed to explore the impact of LLLE on DSS-induced colitis in mice while investigating the potential involvement of gut microbiota and metabolite.

2. Materials and methods

2.1. Materials

LLLE (Leu-Leu-Leu-Glu, molecular weight: 486.60 Da, >98%) was synthesized by Shanghai Chutide Biotechnology Co., Ltd (Shanghai, China).

2.2. Animal experiment design

Seven-week-old BALB/c male mice were obtained from Cavens Experimental Animal (Changzhou, China). After 2 weeks of acclimation with free access to food and water, mice were randomly divided into three groups (n = 8): control group (Normal), DSS-induced group (Model), and peptide treatment group (LLLE). The LLLE group was given 50 mg/kg LLLE solution by gavage daily, and the other groups were given the same amount of carboxymethyl cellulose (CMC) solution. All groups were maintained in control chow diet (Supplementary Table 1) for one week. After one week of intragastric pretreatment, the control group received normal sterile water, while the model and LLLE groups were treated with 2.5% DSS in drinking water for one week to induce colitis. Mice were then euthanized and serum, and tissues were collected. During the entire experiment, body weight and food, and water were recorded every day. The fecal properties, including blood in the stools, were monitored daily during the DSS treatment period. Feces were collected at the beginning and end of the study. The protocol for the animal study was approved by the Animal Research Ethics Committee (UJS-IACUC-2022102802 and IPROTO202300000035).

2.3. Disease activity index (DAI) measurement

During DSS-induced colitis, mice were monitored daily. The DAI score assessed overall disease severity in mice, including weight loss, stool consistency, and blood (hemoccult tests) in the stool (Table 1). The DAI score is calculated as the sum of these three parameters, as in our previous research (Yang et al., 2024).

2.4. Organ index evaluation

Following euthanasia, the liver, spleen, kidney, and colon were collected. The liver, spleen, and kidney indices were calculated as the ratio of each organ weight to the body weight. Additionally, the length of the colon was measured.

2.5. Enzyme-linked immunosorbent assay

After the mice were sacrificed, the collected blood was centrifuged at 3000 r/min for 15 min. IL-6 levels in the serum were measured by using ELISA kits (Beyotime Institute of Biotechnology, PI326).

2.6. Colon histopathological evaluation

After euthanasia, the mice were dissected to isolate the colon tissue, which was then measured. Subsequently, the colon was fixed and stained with hematoxylin and eosin (H&E). Histopathology score is determined based on the severity of inflammatory cell infiltration (0–3), the extent of damage (0–3), and the extent of crypt damage (0–4), which was according to our previous methods (Yang et al., 2024).

2.7. 16S rRNA sequencing

Mouse fecal samples (100–200 mg) were used for DNA extraction following standard procedures. Genomic DNA (30 ng) was then used with fusion primers to set up the PCR reaction system for amplification. The V3-V4 region of the fecal DNA was amplified by PCR utilizing a universal primer. Agilent 2100 Bioanalyzer was utilized to analyze the size distribution and concentration of the library fragments. Sequencing on the HiSeq platform was performed for libraries that met the quality criteria, guided by fragment size. Off-machine data underwent filtering, retaining high-quality, clean data for subsequent analysis. The reads were grouped into tags based on overlapping sequences and clustered into operational taxonomic units (OTUs) according to a predefined similarity threshold. These OTUs were further annotated by comparing them with a reference database to achieve species identification. The OTUs and their corresponding species annotations were analyzed to investigate species complexity within samples and differences between groups. Additionally, the concentration and integrity of the extracted DNA were meticulously evaluated. Representative OTU sequences underwent further taxonomic classification and analysis. The microbial community composition for each sample was calculated across various taxonomic levels, including phylum, class, order, family, genus, and OTUs. Linear discriminant analysis (LDA) effect size (LEfSe) was employed to identify biomarkers within the gut microbiota, with LDA >4 as significant biomarkers utilizing RStudio for data processing and visualization. Alpha diversity and principal coordinate analysis (PCoA) analyses were conducted to visualize gut microbiota diversity, utilizing RStudio for data processing and visualization, as our previous research (Gu et al., 2024; Yang et al., 2024).

2.8. Fecal metabolomic analysis

The stool samples were thawed gradually at 4 °C, and the extraction solution, internal standard, and two small steel beads were added to homogenize the feces. Subsequently, the samples underwent ultrasonication for 10 min at 4 °C and were incubated for 1 h at −20 °C.

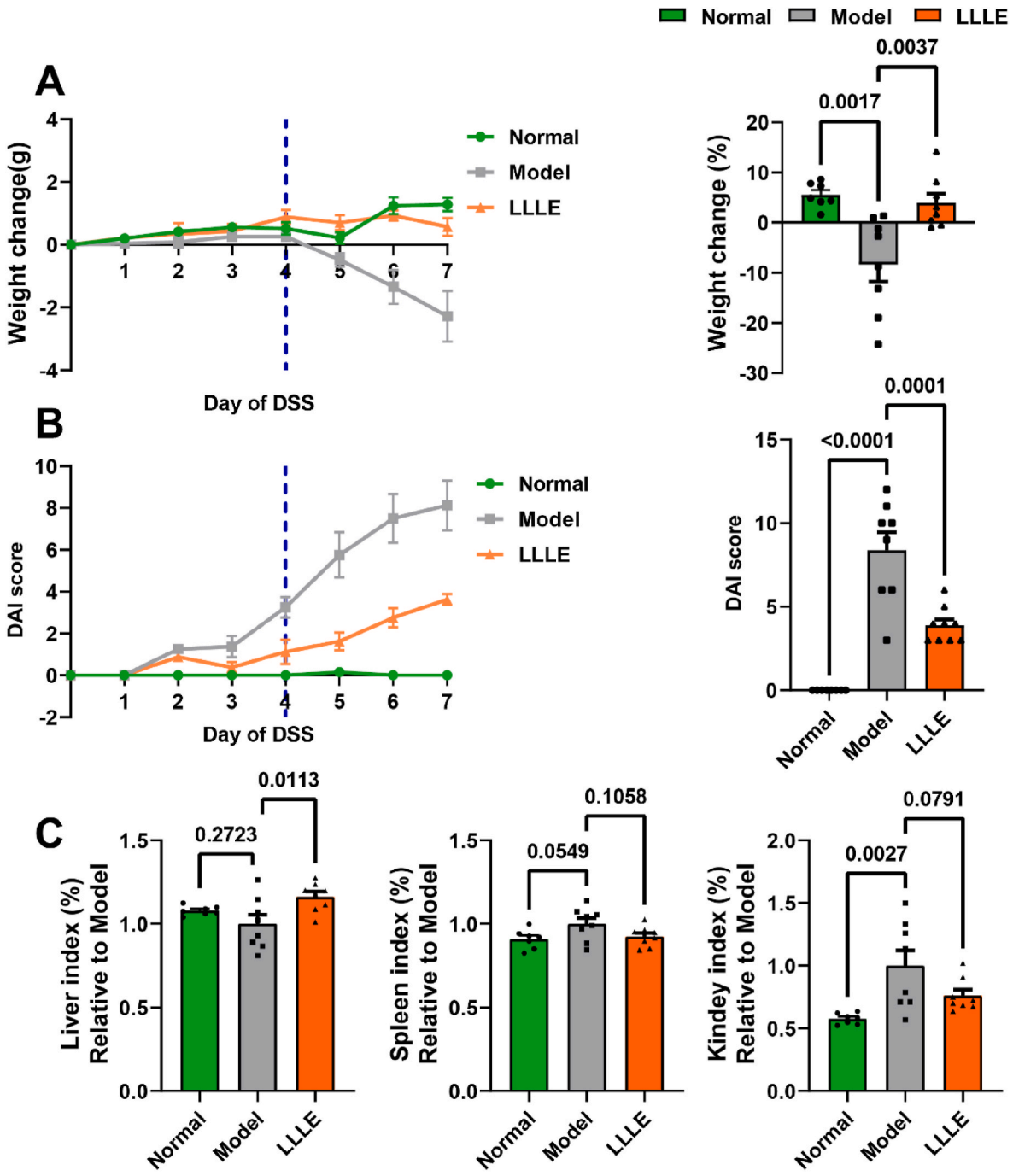

Fig. 1. LLLE alleviated DSS-induced colitis in mice. Mice were treated with 0.5% CMC solution or CA (50 mg/kg bw/day) for 7 days, and colitis was induced with 2.5% DSS solution for the last seven days. (A) The time course for the alteration of body weight and the changes at day 7. (B) The Disease activity index (DAI) time course and the final score at day 7. (C) Organ index measurement post-euthanasia. (A–C) n = 8 per group, data are presented as mean ± SEM, standard error of the mean.

Following centrifugation for 15 min at 4 °C, the supernatant was concentrated using a freeze-dried vacuum system. After reconstitution, the mixture was vortexed for 1 min, ultrasonicated for 10 min at 4 °C, and centrifuged for 15 min at 4 °C. The supernatant was analyzed for metabolite separation and detection, as our previous research (Gu et al., 2024; Yang et al., 2024). To ensure the reliability of the liquid chromatography-mass spectrometry (LC-MS) analysis, 50 μL of supernatant from each sample was meticulously combined with synthetic QC samples, evaluating both repeatability and stability. Mass spectrometric analysis was conducted in positive and negative ion modes using LC–MS/MS QE system (Thermo Fisher Scientific, California, USA). Subsequent peak extraction and metabolite identification will be carried out using the BGI and mzCloud libraries. Key metabolites will be identified based on their fold changes (FC) and variable importance projection (VIP) values utilizing RStudio for data processing and visualization.

2.9. Statistical analysis

Data analysis and graphical representation were conducted using GraphPad Prism 9.0 software. Statistical differences between groups were evaluated using one-way ANOVA followed by Tukey's multiple

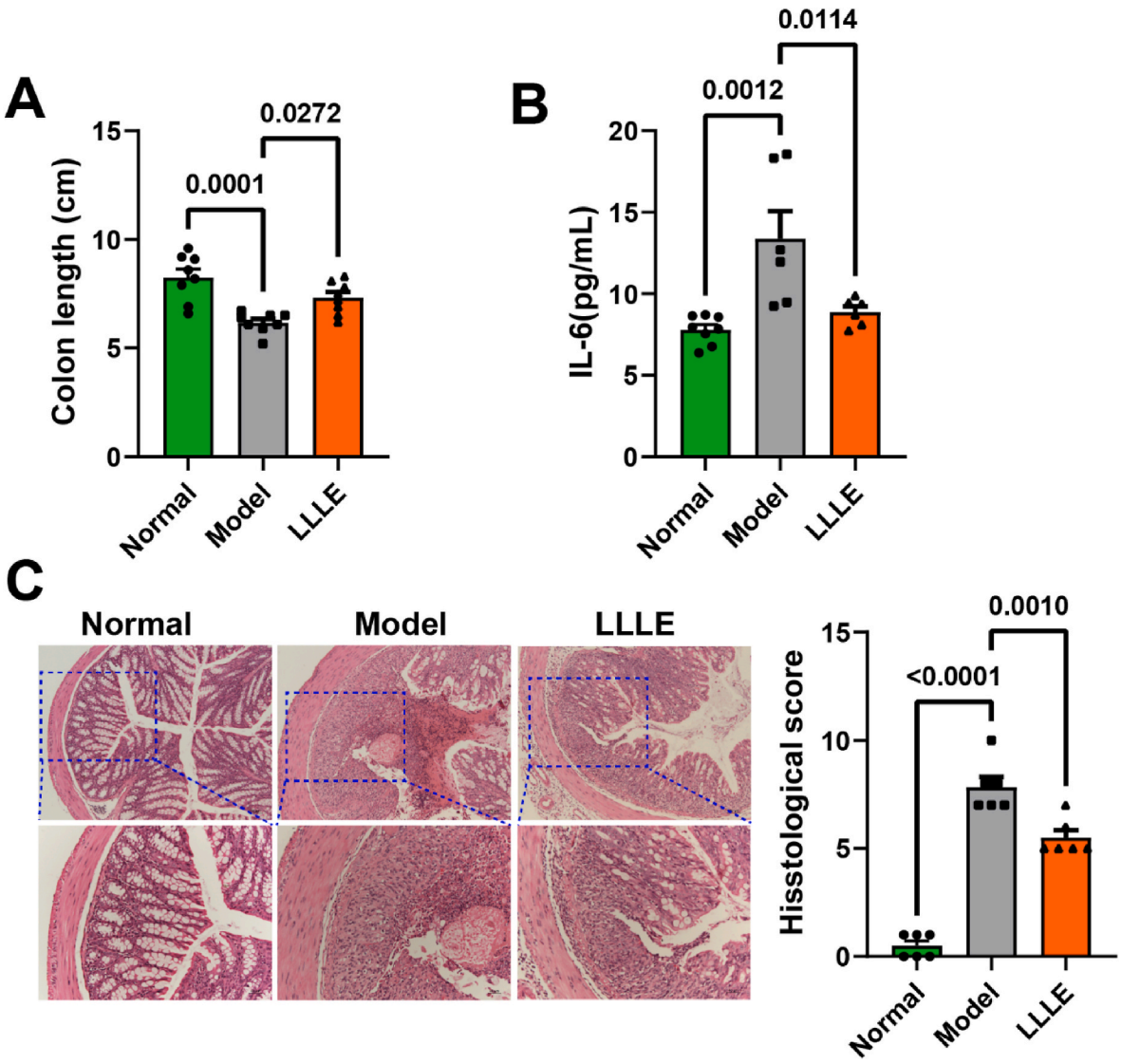

Fig. 2. LLLE mitigates colon tissue damage and inflammation in colitis mice. (A) Colon length measurement post-euthanasia. (B) Expression levels of IL-6 in mouse serum. (C) representative images of H&E staining colon (100 × magnification, 200 × magnification). (A–C) n = 6–8 per group, data are presented as mean ± SEM.

comparison test. Results are presented as mean ± SEM, and $P < 0.05$ was considered statistically significant. For the 16S rRNA sequencing analysis, QIIME 2 was used for microbiome analysis, including diversity analysis, taxonomy assignment, and differential abundance testing. The visualization was based on R 4.3 (phyloseq, vegan, ggplot2, DESeq2, etc). For the fecal metabolite analysis, the visualization was based on R 4.3, including mixOmics, ggplot2, and ComplexHeatmap, etc.

3. Results

3.1. LLLE alleviated DSS-induced weight loss and DAI scores in mice

During the experiment, the body weight of mice in the DSS-induced group (model) started to decline at day 5, reaching significance at days 6 and 7 compared to the normal group ($P = 0.0017$) (Fig. 1A). Supplementation with LLLE notably mitigated the weight loss compared to the model group ($P = 0.037$) (Fig. 1A). DAI scores, calculated based on changes in mouse weight, fecal consistency, and fecal blood content, increased in the model group starting at day 4, compared to the normal group (Fig. 1B). As the days of DSS-induced colitis progressed, DAI scores gradually increased in both the Model and LLLE groups. At day 7, the DAI score in the model group significantly exceeded that of the normal group ($P < 00001$), which was significantly reduced by LLLE treatment ($P = 0.0001$) (Fig. 1B).

3.2. LLLE mitigated DSS-induced inflammatory factors

To investigate the impact of LLLE in inflammation on DSS-induced colitis, we assessed liver, spleen, and kidney indices. DSS treatment increased the kidney ($P = 0.0027$) and spleen ($P = 0.0549$) indices and decreased the liver index ($P = 0.2723$), compared to the normal group (Fig. 1C). LLLE elevated the liver ($P = 0.0113$) index while decreasing spleen ($P = 0.1058$) and kidney ($P = 0.0791$) indices compared to the model group (Fig. 1C). To further investigate the impact of LLLE on the colon of DSS-induced mice, we assessed colon length and conducted histopathological examinations following H&E staining. As shown in Fig. 2A, compared with the normal group, the colon of mice in the model group was significantly shortened ($P = 0.0001$), which was alleviated considerably by LLLE pretreatment, compared to the model group ($P = 0.0272$). To further evaluate the impact of LLLE on inflammation, we measured the expression of the pro-inflammatory cytokine IL-6 in the serum of mice from all experimental groups. As shown in Fig. 2B, IL-6 expression was significantly higher in the serum of DSS-treated mice compared to the normal group ($P = 0.0012$). LLLE supplementation

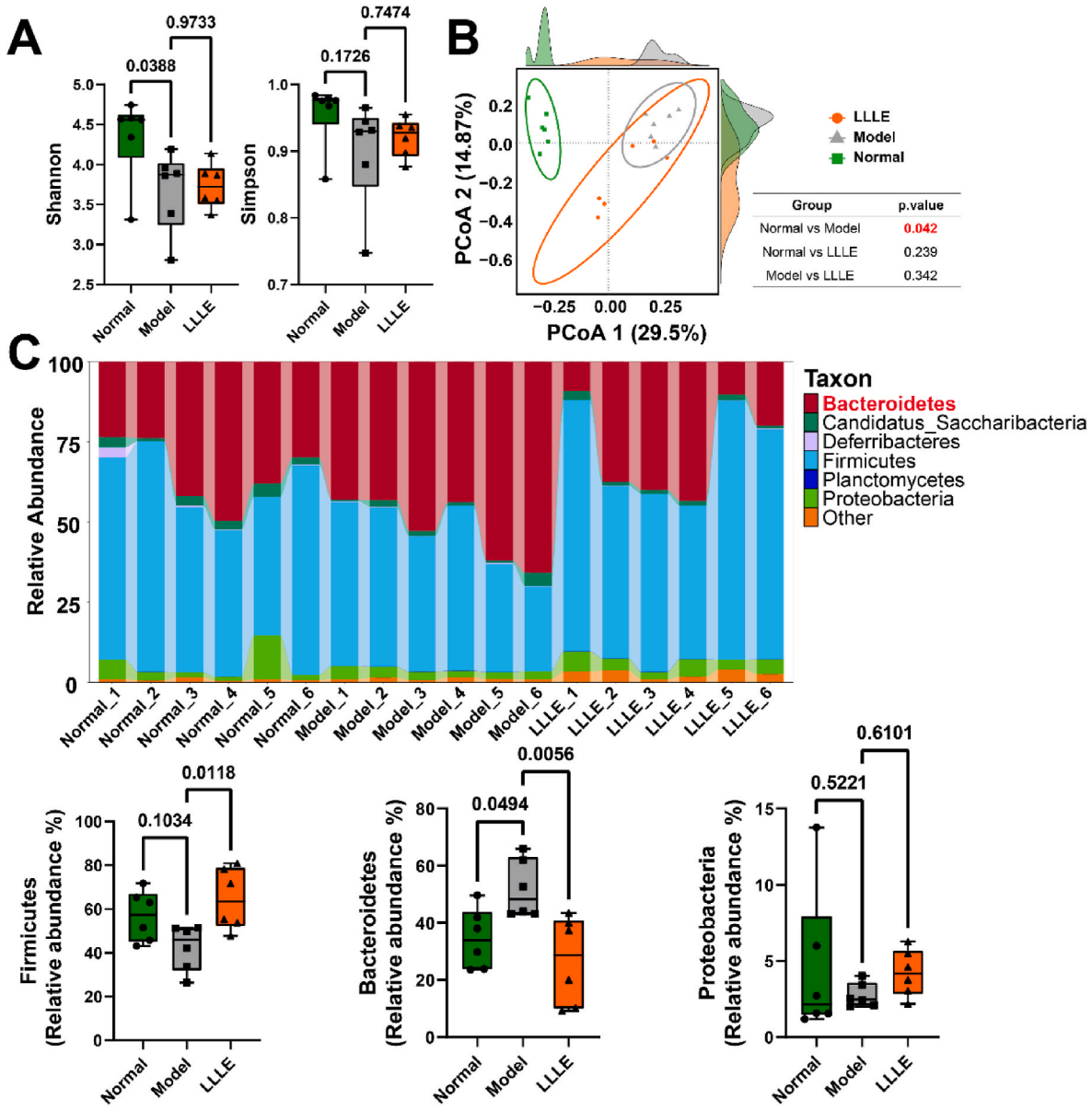

Fig. 3. LLLE modulates the diversity of the gut microbiota. (A) α-diversity. (B) PCoA of operational taxonomic units (OTUs). (C) The relative abundance of microbial taxa at phylum levels. (A–C) n = 6 per group, data are presented as mean ± SEM.

notably reduced IL-6 levels ($P = 0.0014$), compared to the model group (Fig. 2B). As shown in Fig. 2C, the colon tissue structure of the mice in the normal group was healthy with numerous goblet cells, intact crypt structure, and no apparent inflammatory cell infiltration. However, mice in the model group exhibited abnormal colon tissue structure, crypt loss, inflammatory cell infiltration, severe mucosal damage, and significantly elevated histological scores ($P < 0.0001$), compared to the normal group (Fig. 2C). Compared to the model group, LLLE treatment significantly alleviated crypt damage, diminished mucosal injury, less infiltration of inflammatory cells, and markedly lower histological scores ($P = 0.001$) (Fig. 2C).

3.3. LLLE modified the composition of gut microbiota in mice suffering from DSS-induced colitis

The 16S rRNA sequencing analysis was used to explore the potential modulation of LLLE on gut microbiota. Shannon and Simpson indices were employed to evaluate microbial diversity. Fig. 3A showed that the Shannon index significantly decreased in the model group compared to the normal group ($P = 0.0388$). LLLE did not reverse the changes in Shannon index caused by DSS ($P = 0.977$). No significant differences were seen in the Simpson, Richness, Chao, and ACE indices for any group (Fig. 3A, and Supplementary Fig. 1). In our analysis, the PCoA revealed that the gut microbiota of subjects was organized into distinct clusters (Fig. 3B), indicating significant differences in microbial community composition among groups. Notably, a clear separation was observed between the normal and model groups, suggesting that the gut microbiota profiles are influenced by the inflammatory conditions in the model group ($P = 0.042$). LLLE intervention partially mitigated DSS-induced alterations ($P = 0.342$), positioning it between the normal and model groups (Fig. 3B). Fig. 3C shows the gut microiota composition at the phylum level of each group of mice. Six types of gut bacteria were detected at the phylum level, including *Firmicutes*, *Bacteroidetes*, *Proteobacteria*, *Candidatus_Saccharibacteria*, *Deferribacteres*, *Planctomycetes*, and others. Among them, *Firmicutes* and *Bacteroidetes* are the dominant bacterial groups at the phylum level. As shown in Fig. 3C, the relative abundance of *Firmicutes* decreased after DSS administration ($P = 0.1034$), which was alleviated to normal levels by LLLE pretreatment (P

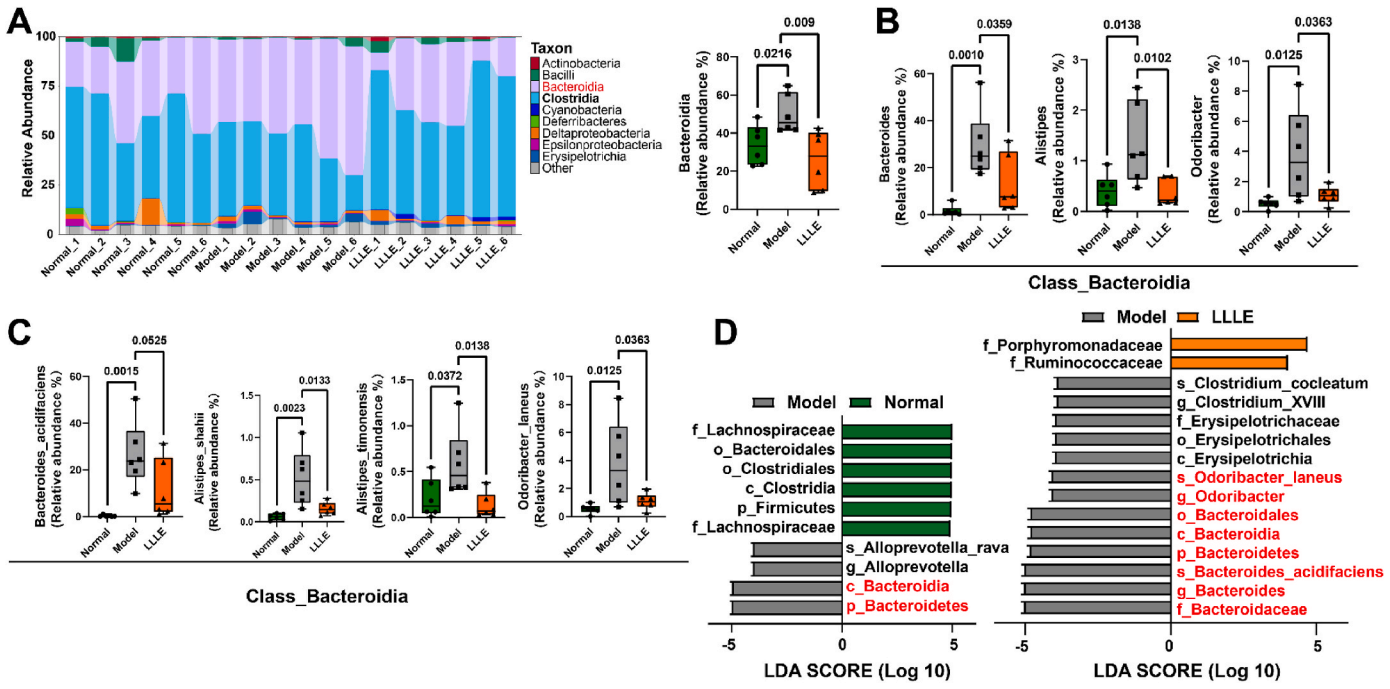

Fig. 4. LLLE alters the composition of gut microbiota. (A) The relative abundance of microbial taxa at class levels. (B) The relative abundance of microbial taxa of *Bacteroidia* at genus levels. (C) The relative abundance of microbial taxa of *Bacteroidia* at species levels. (D) The LDA score assessed taxonomic importance in gut microbiota, LDA >4. (A–C) n = 6 per group, data are presented as mean ± SEM.

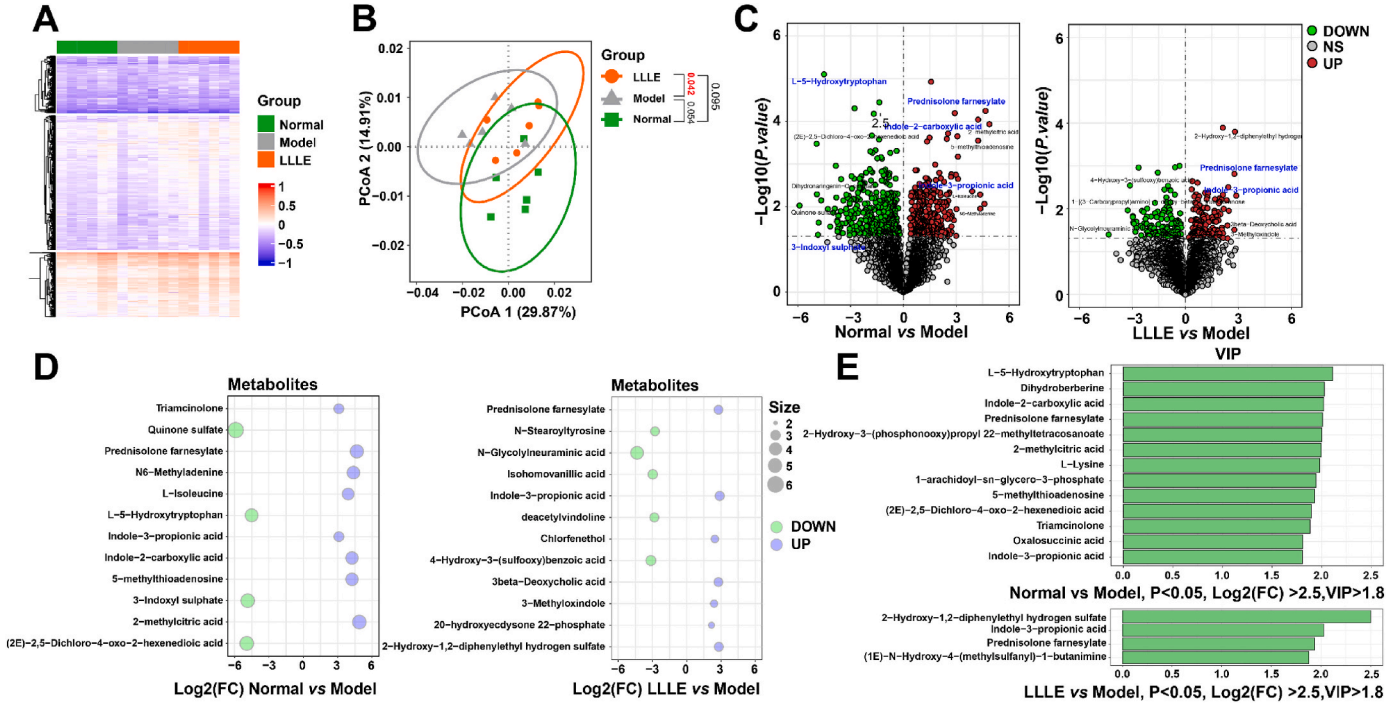

Fig. 5. LLLE alters the metabolites of feces. (A) The heatmap of fecal metabolites. (B) PCoA of fecal metabolites. (C) Volcano plots of serum metabolites. (D) The crucial metabolites exhibited significant fold changes. (E) The VIP score assesses metabolite importance in fecal samples. (A–C) n = 6 per group, data are presented as mean ± SEM.

= 0.0118). Meanwhile, the relative abundance of *Bacteroidetes* increased significantly after DSS administration (P = 0.0494), while LLLE pre-treatment protected it at normal levels (P = 0.0056), compared to model group (Fig. 3C). Fig. 4A revealed the composition of gut microbiota at the class level. Compared to the normal group, there was a significant increase in the relative abundance of *Bacteroidia* in the model group (P = 0.0216), and supplementation with LLLE significantly reversed this trend (P = 0.009). Moreover, compared to the normal group, the model group exhibited a significant increase in the relative abundance of the genera of *Bacteroides* (P = 0.0010), *Alistipes* (P = 0.0138) and *Odoribacter* (P = 0.0125) (Fig. 4B). However, LLLE supplementation significantly reversed these changes (P = 0.0359, P = 0.0102, P = 0.0363), compared

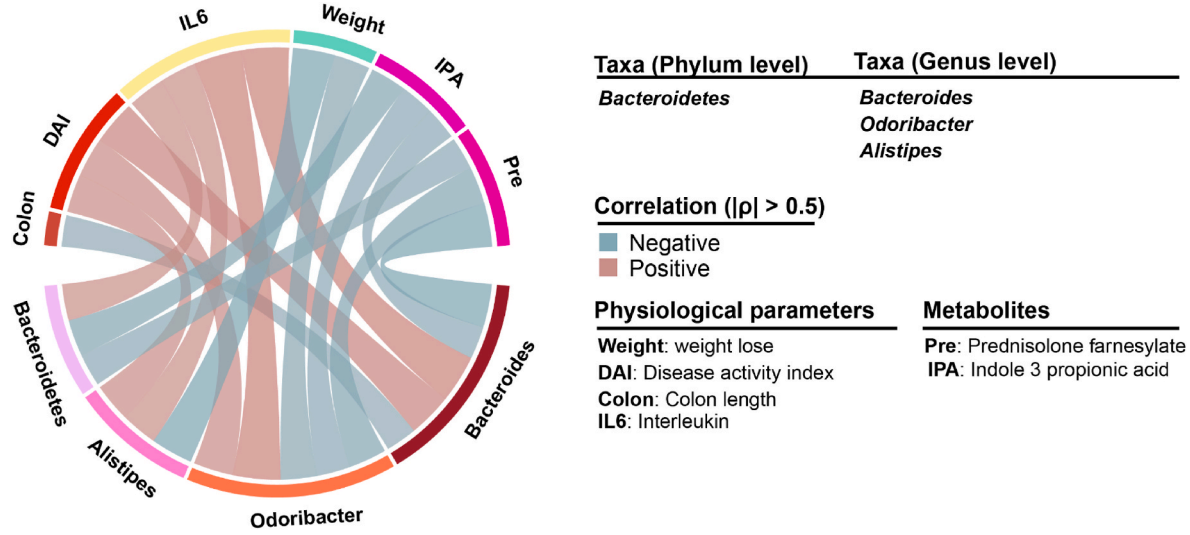

Fig. 6. Correlation analysis among the significant difference genera ($P < 0.05$), crucial metabolites, and physiological parameters ($|\rho| > 0.5$, $P < 0.05$).

to model group (Fig. 4B). At the species levels, compared with the normal group, the relative abundance of *Bacteroides acidifaciens* ($P = 0.0015$), *Alistipes shahii* ($P = 0.0023$), *Alistipes timonensis* ($P = 0.0372$), and *Odoribacter laneus* ($P = 0.0125$) significantly increased in the model group (Fig. 4C). Supplementation with LLLE significantly reversed this alteration compared with the model group ($P = 0.0525$, $P = 0.0133$, $P = 0.0138$, $P = 0.0363$) (Fig. 4C). The LEfSe indicated the enrichment of bacteria belonging to the phylum *Bacteroidetes* in the model group (Fig. 4D), compared to normal and LLLE groups.

3.4. LLLE altered fecal metabolites in DSS-induced colitis mice

Next, we measured gut-derived metabolites to identify a protective metabolite that could be upregulated or disease-promoting metabolites that could be reduced by LLLE. The heatmap showed the content of fecal metabolites in each group (Fig. 5A). PCoA was performed between each two groups to identify the relationship between metabolite expression and sample category (Fig. 5B). Cluster analysis of differential metabolite expression levels showed significant changes after DSS exposure and LLLE intervention. After DSS exposure, a significant separation between the model and normal group was observed ($P = 0.042$), with the LLLE intervention situated between the normal and model groups ($P = 0.054$ and 0.095) (Fig. 5B). Differential metabolites were screened according to the following conditions: 1) VIP $\geq$1.8 in the Orthogonal partial least squares-discriminant analysis (OPLS-DA) model, and 2) Log2 (FC) ≥ 2.5 or ≤ -2.5), 3) $P < 0.05$. Fig. 5C shows the different metabolite comparisons between the normal and model groups. Compared to the model group, 298 metabolites were up-regulated, and 377 metabolites were down-regulated in the normal group (Fig. 5C). Compared with the model group, the LLLE intervention upregulated 150 metabolites and down-regulated 139 metabolites (Fig. 5C). The mice in normal group had significant lower levels of L-5-Hydroxytryptophan (Log2 (FC) $= -4.51$, $P < 0.001$), and 3-indoxyl sulfate (Log2 (FC) $= -4.85$, $P < 0.001$) in feces (Fig. 5D), compared with the model group. Meanwhile, there was significant high-level content of several metabolites, including prednisolone farnesylate (Log2 (FC) $= 4.66$, $P < 0.001$), indole-2-carboxylic acid (Log2 (FC) $= 4.24$, $P < 0.001$) and indole-3-propionic acid (Log2 (FC) $= 3.1$, $P = 0.002$) in the feces of the normal group compared to the model group (Fig. 5D). The supplementation with LLLE markedly attenuated the alteration trends in prednisolone farnesylate (Log2 (FC) $= 2.78$, $P = 0.002$) and indole-3-propionic acid (Log2 (FC) $= 2.88$, $P = 0.005$) in feces, compared with the model group (Fig. 5D). Meanwhile, the supplementation with LLLE markedly decreased the content of N-glycolylneuraminic acid (Log2 (FC) $= -4.33$, $P = 0.039$) and 4-hydroxy-3-(sulfooxy) benzoic acid (Log2 (FC) $= -3{,}13$, $P = 0.002$) in feces, compared with the model group (Fig. 5D). Furthermore, the VIP analysis also showed the crucial metabolites including prednisolone farnesylate and indole-3-propionic acid with the LLLE intervention (Fig. 5E).

3.5. LLLE alleviated inflammation by regulating gut microbiota and gut metabolites in DSS-induced colitis mice

The Spearman correlation network analysis revealed the intricate relationships among the gut microbiota, metabolome, and host physiological responses during LLLE intervention. The genera, including *Bacteroidetes*, *Odoribacter*, and *Alistipes*, correlated negatively with the indicators of weight loss, and colon length, prednisolone farnesylate, and indole-3-propionic acid (Fig. 6). Conversely, *Bacteroidetes*, *Odoribacter*, and *Alistipes* showed a positive correlation with IL6 and DAI (Fig. 6).

4. Discussion

In our study, LLLE supplementation alleviated DSS-induced weight loss, colon shortening, DAI and histopathology scores, as well as IL6 levels. These results suggest that LLLE is effective in ameliorating colitis. In addition, 16srRNA sequencing and untargeted metabolomics results further demonstrated that LLLE has potential to ameliorate colitis by modulating the gut microbiota and fecal metabolites.

Recently, protein hydrolysates have attracted considerable attention due to their biological activities, especially bioactive peptides, which promise to enhance human health and mitigate disease risks. Our previous research supports the link between sturgeon by-products and a spectrum of diseases, such as obesity, IBD, and osteoporotic (Gao et al., 2020, 2023, 2024). Chondroitin sulfate has shown efficacy in improving insulin resistance and colorectal cancer via modulating the gut microbiota (Gao et al., 2023; Wu et al., 2022), suggesting the potential benefits of sturgeon by-products. The antioxidant peptides derived from sturgeon ovaries possess antiosteoporotic properties in oxidative-stressed MC3T3-E1 cells (Gao et al., 2024). Our previous study discovered that purified sturgeon peptide exhibits anti-inflammatory effects (Gao et al., 2021; Yuan et al., 2021). The peptide LLLE, isolated from ethanol-solubilized cartilage hydrolysate, decreased NO and IL-6 production while increasing IL-10 expression (Yuan et al., 2023). Extensive research has firmly established a significant association between UC and the gut microbiota, highlighting the potential benefits of altering microbiota composition to relieve UC symptoms (Świrkosz

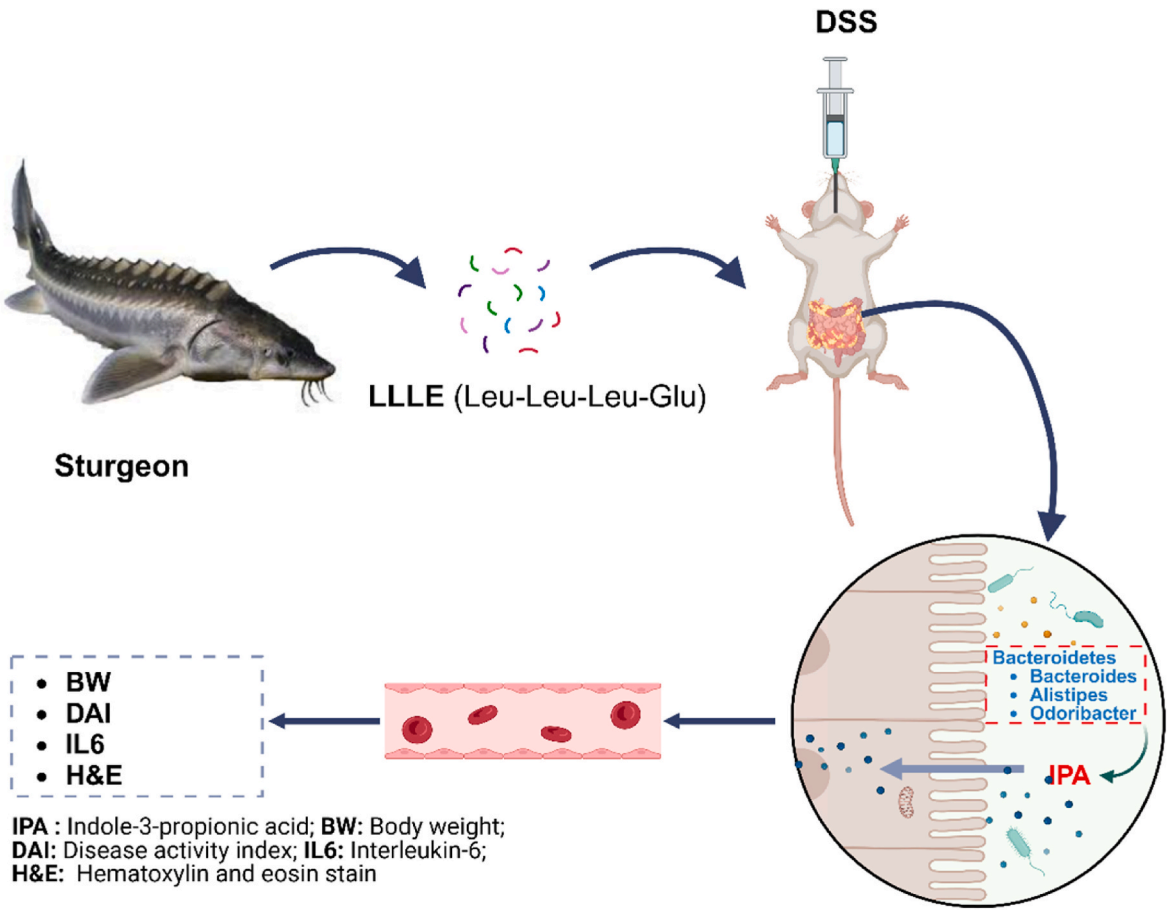

Fig. 7. Mechanism of the sturgeon-derived peptide (LLLE: Leu-Leu-Leu-Glu) in mitigating colitis in mice.

et al., 2023). Our previous study revealed that sturgeon hydrolysates might mitigate DSS-induced colitis by modifying gut microbiota composition (Gao et al., 2020), which is consistent with our result that sturgeon peptide LLLE prevented DSS-induced colitis with anti-inflammatory efficacy and LLLE alleviates the enhancement of *Bacteroidetes* induced by DSS treatment. Previous studies have indicated that UC involves infiltrating neutrophils and macrophages into the colon mucosa, resulting in significant secretion of inflammatory cytokines and exacerbating the inflammatory condition (Műzes et al., 2012). Our results showed that LLLE alleviated the DSS-induced inflammatory cell infiltration.

In the Trinitrobenzene sulfonic acid (TNBS)-induced colitis model, microbiome analysis indicated an augmentation of overall *Bacteroidetes* at the phylum level (Busbee et al., 2020; Zheng et al., 2017). Researchers observed a notable augmentation in the DSS-induced colitis model in *Bacteroidales* (Lucke et al., 2006; Schwab et al., 2014). The mucosal tissue of patients with ulcerative colitis (UC) harbors a significantly higher abundance of *Bacteroides_spp*, compared to healthy individuals (Lucke et al., 2006). *Bacteroides acidifaciens*, characterized as obligately anaerobic, non-sporing, non-motile gram-negative rods, has been recognized for its capability to degrade protective mucus in the colon and its pro-inflammatory properties (Berry et al., 2013; Staley et al., 2023). Furthermore, a previous study highlights an increase in *Bacteroides acidifaciens* during DSS-induced colitis (Busbee et al., 2020; Schwab et al., 2014), and colonization by *Bacteroides acidifaciens* may induce colitis symptoms by polarizing T helper cell differentiation (Staley et al., 2023; He et al., 2022). Comparatively, conventional C57BL/6 mice given a high oral dose of *Bacteroides acidifaciens* exhibited more severe colitis symptoms than the healthy group, which suggests that *Bacteroides acidifaciens* may have the potential to induce colitis upon reaching pathogenic thresholds (He et al., 2022; Staley et al., 2023). This aligns with our findings, where DSS treatment increased the abundance of *Bacteroides acidifaciens*, while supplementation with LLLE significantly mitigated this upward trend.

Previous research has demonstrated that elevating luminal indole propionic acid levels can increase serum and tissue indole propionic acid levels (Dodd et al., 2017; Flannigan et al., 2023). Following recovery from DSS-induced colitis, microbiota depletion significantly exacerbated intestinal fibrosis and inflammation, while the administration of indole-3-propionic acid markedly alleviated both conditions (Flannigan et al., 2023). Indole propionic acid exhibits enhanced ability to cross the blood-brain barrier, travel to target organs via the circulatory system, activate specific receptors, and engage in the host physiological processes, potentially influencing overall health through pathways including the gut-brain, gut-liver, and gut-lung axes (Jiang et al., 2022). Our study found that DSS significantly reduced the content of fecal indole-3-propionic acid. However, the LLLE supplementation significantly reversed the decline in indole-3-propionic acid levels. Indole and its derivatives inhibit the production of proinflammatory cytokines such as monocyte chemoattractant protein-1 (MCP-1), tumor necrosis factor-alpha (TNF-α), interleukin-1 beta (IL-1β), and IL-6 (Du et al., 2021; Garcez et al., 2020; Zhao et al., 2019), and exert potent anti-inflammatory effects by activating Pregnane X receptor (PXR) and Aryl hydrocarbon receptor (AhR), which regulate immune system function and are crucial for enhancing intestinal health (Alexeev et al., 2018; Venkatesh et al., 2014). In our findings, LLLE significantly counteracted the DSS-induced reduction of serum IL6 by likely enhancing indole propionic acid production in the feces, which enters the body through the circulatory system. This benefits individuals with inflammatory bowel disease, hemorrhagic colitis, and colorectal cancer,

thereby promoting overall human health.

5. Conclusion

In summary, sturgeon polypeptide LLLE shows promise in alleviating UC symptoms by inhibiting the overexpression of inflammatory factors induced by DSS colitis. Its anti-inflammatory effects may involve the downregulation of an excessive abundance of *Bacteroides*. Simultaneously, alterations in gut microbiota contribute to increased fecal metabolite indole-3-propionic acid levels, further suppressing inflammatory factor expression (Fig. 7). Sturgeon polypeptides represent a promising and safer dietary intervention for alternative approaches to prevent or treat colonic inflammation. Future research should focus on elucidating the underlying molecular mechanisms of LLLE, particularly its effects in female models, as only male mice were used in this study. Understanding potential gender differences in response to sturgeon peptides will be crucial for developing effective treatments. Additionally, exploring the development of new anti-inflammatory sturgeon polypeptide products could provide further therapeutic options.

CRediT authorship contribution statement

Jie Lin: wrote the paper draft, performed the experiments. **Jiani Yang:** performed the experiments, All data were generated in-house, and no paper mill was used, All authors agree to be accountable for all aspects of work, ensuring integrity and accuracy. **Leqi Cui:** corrected the draft. **Ravinder Nagpal:** corrected the draft. **Prashant Singh:** corrected the draft. **Gloria Salazar:** corrected the draft. **Qinchun Rao:** corrected the draft. **Ye Peng:** corrected the draft, supervised the experimentation. **Quancai Sun:** corrected the draft, supervised the experimentation.

Consent for publication

The authors declare that there are no competing interests.

Declaration of competing interest

No conflict of interest is associated with the current manuscript. Declarations of Ethics approval and consent to participate.

Appendix A. Supplementary data

Supplementary data to this article can be found online at https://doi.org/10.1016/j.crfs.2024.100898.

Data availability

Data will be made available on request.

References

Alexeev, E.E., Lanis, J.M., Kao, D.J., Campbell, E.L., Kelly, C.J., Battista, K.D., Gerich, M. E., Jenkins, B.R., Walk, S.T., Kominsky, D.J., Colgan, S.P., 2018. Microbiota-derived indole metabolites promote human and murine intestinal homeostasis through regulation of interleukin-10 receptor. Am. J. Pathol. 188, 1183–1194. https://doi.org/10.1016/j.ajpath.2018.01.011.

Berry, D., Stecher, B., Schintlmeister, A., Reichert, J., Brugiroux, S., Wild, B., Wanek, W., Richter, A., Rauch, I., Decker, T., Loy, A., Wagner, M., 2013. Host-compound foraging by intestinal microbiota revealed by single-cell stable isotope probing. Proc. Natl. Acad. Sci. USA 110, 4720–4725. https://doi.org/10.1073/pnas.1219247110.

Busbee, P.B., Menzel, L., Alrafas, H.R., Dopkins, N., Becker, W., Miranda, K., Tang, C., Chatterjee, S., Singh, U., Nagarkatti, M., Nagarkatti, P.S., 2020. Indole-3-carbinol prevents colitis and associated microbial dysbiosis in an IL-22-dependent manner. JCI. Insight. 5. https://doi.org/10.1172/jci.insight.127551.

Dodd, D., Spitzer, M.H., Van Treuren, W., Merrill, B.D., Hryckowian, A.J., Higginbottom, S.K., Le, A., Cowan, T.M., Nolan, G.P., Fischbach, M.A., Sonnenburg, J.L., 2017. A gut bacterial pathway metabolizes aromatic amino acids into nine circulating metabolites. Nature 551, 648–652. https://doi.org/10.1038/nature24661.

Du, L., Qi, R., Wang, J., Liu, Z., Wu, Z., 2021. Indole-3-propionic acid, a functional metabolite of Clostridium sporogenes, promotes muscle tissue development and reduces muscle cell inflammation. Int. J. Mol. Sci. 22, 12435. https://doi.org/10.3390/ijms222212435.

Flannigan, K.L., Nieves, K.M., Szczepanski, H.E., Serra, A., Lee, J.W., Alston, L.A., Ramay, H., Mani, S., Hirota, S.A., 2023. The Pregnane X receptor and indole-3-propionic acid shape the intestinal mesenchyme to restrain inflammation and fibrosis. Cell. Mol. Gastroenterol. Hepatol. 15, 765–795. https://doi.org/10.1016/j.jcmgh.2022.10.014.

Gao, R., Qi, Z., Lin, J., Wang, G., Chen, G., Yuan, L., Sun, Q., 2023. Chondroitin sulfate alleviated obesity by modulating gut microbiota and liver metabolome in high-fat-diet-induced obese mice. J. Agric. Food Chem. 71, 9419–9428. https://doi.org/10.1021/acs.jafc.3c02642.

Gao, R., Shen, Y., Shu, W., Jin, W., Bai, F., Wang, J., Zhang, Y., El-Seedi, H., Sun, Q., Yuan, L., 2020. Sturgeon hydrolysates alleviate DSS-induced colon colitis in mice by modulating NF-κB, MAPK, and microbiota composition. Food Funct. 11, 6987–6999. https://doi.org/10.1039/c9fo02772f.

Gao, R., Zhu, L., Zhang, W., Jin, W., Bai, F., Xu, P., Wang, J., Sun, Q., Guo, Z., Yuan, L., 2024. Novel peptides from sturgeon ovarian protein hydrolysates prevent oxidative stress-induced dysfunction in osteoblast cells: purification, identification, and characterization. J. Agric. Food Chem. 72, 10076–10088. https://doi.org/10.1021/acs.jafc.3c07021.

Gao, R.C., Shu, W.H., Shen, Y., Sun, Q.C., Jin, W.G., Li, D.J., Li, Y., Yuan, L., 2021. Peptide fraction from sturgeon muscle by pepsin hydrolysis exerts anti-inflammatory effects in LPS-stimulated RAW264.7 macrophages via MAPK and NF-κB pathways. Food Sci. Hum. Wellness 10, 103–111. https://doi.org/10.1016/j.fshw.2020.04.014.

Garcez, M.L., Tan, V.X., Heng, B., Guillemin, J.G., 2020. Sodium butyrate and indole-3-propionic acid prevent the increase of cytokines and kynurenine levels in LPS-induced human primary astrocytes. Int. J. Tryptophan Res. 13, 1178646920978404. https://doi.org/10.1177/1178646920978404.

Ghouri, Y.A., Tahan, V., Shen, B., 2020. Secondary causes of inflammatory bowel diseases. World J. Gastroenterol. 26, 3998–4017. https://doi.org/10.3748/wjg.v26.i28.3998.

Gu, T., Lin, J., Yang, J., Mumby, W., Sun, Q., Peng, Y., 2024. Chlorantraniliprole exposure aggravates high-fat diet-induced metabolic disorders in mice by regulating gut microbiota and its metabolites. Food Sci. Hum. Wellness. https://doi.org/10.26599/FSHW.2024.9250079.

He, R., Chen, J., Zhao, Z., Shi, C., Du, Y., Yi, M., Feng, L., Peng, Q., Cui, Z., Gao, R., Wang, H., Huang, Y., Liu, Z., Wang, C., 2022. T-cell activation Rho GTPase-activating protein maintains intestinal homeostasis by regulating intestinal T helper cells differentiation through the gut microbiota. Front. Immunol. 13, 1030947. https://doi.org/10.3389/fmicb.2022.1030947.

Hoon, L.S., Kwon, J.e., Cho, M.-L., 2018. Immunological pathogenesis of inflammatory bowel disease. Int. Res. 16, 26–42. https://doi.org/10.5217/ir.2018.16.1.26.

Jiang, H., Chen, C., Gao, J., 2022. Extensive summary of the important roles of indole propionic acid, a gut microbial metabolite in host health and disease. Nutrients 15. https://doi.org/10.3390/nu15010151.

Knox, N.C., Forbes, J.D., Peterson, C.-L., Van Domselaar, G., Bernstein, C.N., 2019. The gut microbiome in inflammatory bowel disease: lessons learned from other immune-mediated inflammatory diseases. Am. J. Pathol. 114, 1051–1070. https://doi.org/10.14309/ajg.0000000000000305.

Lucke, K., Miehlke, S., Jacobs, E., Schuppler, M., 2006. Prevalence of Bacteroides and Prevotella spp. in ulcerative colitis. J. Med. Microbiol. 55, 617–624. https://doi.org/10.1099/jmm.0.46198-0.

Matsuoka, K., Kanai, T., 2015. The gut microbiota and inflammatory bowel disease. Semin. Immunopathol. 37, 47–55. https://doi.org/10.1007/s00281-014-0454-4.

Műzes, G., Molnár, B., Tulassay, Z., Sipos, F., 2012. Changes of the cytokine profile in inflammatory bowel diseases. World J. Gastroenterol. 18, 5848–5861. https://doi.org/10.3748/wjg.v18.i41.5848.

Nagao-Kitamoto, H., Shreiner, A.B., Gillilland 3rd, M.G., Kitamoto, S., Ishii, C., Hirayama, A., Kuffa, P., El-Zaatari, M., Grasberger, H., Seekatz, A.M., Higgins, P.D., Young, V.B., Fukuda, S., Kao, J.Y., Kamada, N., 2016. Functional characterization of inflammatory bowel disease-associated gut dysbiosis in gnotobiotic mice. Cell. Mol. Gastroenterol. Hepatol. 2, 468–481. https://doi.org/10.1016/j.jcmgh.2016.02.003.

Sartor, R.B., Wu, G.D., 2017. Roles for intestinal bacteria, viruses, and fungi in pathogenesis of inflammatory bowel diseases and therapeutic approaches. Gastroenterology 152, 327. https://doi.org/10.1053/j.gastro.2016.10.012.

Schwab, C., Berry, D., Rauch, I., Rennisch, I., Ramesmayer, J., Hainzl, E., Heider, S., Decker, T., Kenner, L., Müller, M., Strobl, B., Wagner, M., Schleper, C., Loy, A., Urich, T., 2014. Longitudinal study of murine microbiota activity and interactions with the host during acute inflammation and recovery. ISME J. 8, 1101–1114. https://doi.org/10.1038/ismej.2013.223.

Shaik, M.I., Sarbon, N.M., 2022. A review on purification and characterization of anti-proliferative peptides derived from fish protein hydrolysate. Food Rev. Int. 38, 1389–1409. https://doi.org/10.1080/87559129.2020.1812634.

Staley, S.C., Busbee, P.B., Nagarkatti, M., Nagarkatti, P.S., 2023. Role of Bacteroides acidifaciensin gut inflammation during colitis. J. Immunol. 210, 82.19. https://doi.org/10.4049/jimmunol.210.Supp.82.19%JTheJournalofImmunology, 82.19.

Świrkosz, G., Szczygieł, A., Logoń, K., Wrześniewska, M., Gomułka, K., 2023. The role of the microbiome in the pathogenesis and treatment of ulcerative colitis-A literature review. Biomedicines 11. https://doi.org/10.3390/biomedicines11123144.

Teckchandani, S., Nagana Gowda, G.A., Raftery, D., Curatolo, M., 2021. Metabolomics in chronic pain research. Eur. J. Pain 25, 313–326. https://doi.org/10.1002/ejp.1677.

Venkatesan, J., Anil, S., Kim, S.K., Shim, M.S., 2017. Marine fish proteins and peptides for cosmeceuticals: a review. Mar. Drugs 15. https://doi.org/10.3390/md15050143.

Venkatesh, M., Mukherjee, S., Wang, H., Li, H., Sun, K., Benechet, A.P., Qiu, Z., Maher, L., Redinbo, M.R., Phillips, R.S., Fleet, J.C., Kortagere, S., Mukherjee, P., Fasano, A., Le Ven, J., Nicholson, J.K., Dumas, M.E., Khanna, K.M., Mani, S., 2014. Symbiotic bacterial metabolites regulate gastrointestinal barrier function via the xenobiotic sensor PXR and Toll-like receptor 4. Immunity 41, 296–310. https://doi.org/10.1016/j.immuni.2014.06.014.

Wu, R., Shen, Q., Li, P., Shang, N., 2022. Sturgeon chondroitin sulfate restores the balance of gut microbiota in colorectal cancer bearing mice. Int. J. Mol. Sci. 23. https://doi.org/10.3390/ijms23073723.

Yaghoubzadeh, Z., Peyravii Ghadikolaii, F., Kaboosi, H., Safari, R., Fattahi, E., 2020. Antioxidant activity and anticancer effect of bioactive peptides from rainbow trout (Oncorhynchus mykiss) skin hydrolysate. Int. J. Pept. Res. Therapeut. 26, 625–632. https://doi.org/10.1007/s10989-019-09869-5.

Yang, J., Lin, J., Gu, T., Sun, Q., Xu, W., Peng, Y., 2024. Chicoric acid effectively mitigated dextran sulfate sodium (DSS)-Induced colitis in BALB/c mice by modulating the gut microbiota and fecal metabolites. Int. J. Mol. Sci. 25. https://doi.org/10.3390/ijms25020841.

Yuan, L., Chu, Q., Wu, X., Yang, B., Zhang, W., Jin, W., Gao, R., 2021. Anti-inflammatory and antioxidant activity of peptides from ethanol-soluble hydrolysates of sturgeon (Acipenser schrenckii) cartilage. Front. Nutr. 8. https://doi.org/10.3389/fnut.2021.689648.

Yuan, L., Chu, Q., Yang, B., Zhang, W., Sun, Q., Gao, R., 2023. Purification and identification of anti-inflammatory peptides from sturgeon (Acipenser schrenckii) cartilage. Food Sci. Hum. Wellness 12, 2175–2183. https://doi.org/10.1016/j.fshw.2023.03.030.

Zhao, Z.-H., Xin, F.-Z., Xue, Y., Hu, Z., Han, Y., Ma, F., Zhou, D., Liu, X.-L., Cui, A., Liu, Z. J.E., Medicine, M., 2019. Indole-3-propionic acid inhibits gut dysbiosis and endotoxin leakage to attenuate steatohepatitis in rats. Exp. Mol. Med. 51, 1–14. https://doi.org/10.1038/s12276-019-0304-5.

Zheng, H., Chen, M., Li, Y., Wang, Y., Wei, L., Liao, Z., Wang, M., Ma, F., Liao, Q., Xie, Z., 2017. Modulation of gut microbiome composition and function in experimental colitis treated with sulfasalazine. Front. Immunol. 8, 1703. https://doi.org/10.3389/fmicb.2017.01703.